



**HAL**  
open science

# Space charge measurement at solid/liquid interface by PWP method

V. Berry, P. Leblanc, S. Holé, T. Paillat

► **To cite this version:**

V. Berry, P. Leblanc, S. Holé, T. Paillat. Space charge measurement at solid/liquid interface by PWP method. *Journal of Electrostatics*, 2024, 128, pp.103894. 10.1016/j.elstat.2024.103894. hal-04393866

**HAL Id: hal-04393866**

**<https://hal.science/hal-04393866>**

Submitted on 15 Jan 2024

**HAL** is a multi-disciplinary open access archive for the deposit and dissemination of scientific research documents, whether they are published or not. The documents may come from teaching and research institutions in France or abroad, or from public or private research centers.

L'archive ouverte pluridisciplinaire **HAL**, est destinée au dépôt et à la diffusion de documents scientifiques de niveau recherche, publiés ou non, émanant des établissements d'enseignement et de recherche français ou étrangers, des laboratoires publics ou privés.

# Space charge measurement at solid/liquid interface by PWP method

V. Berry<sup>1</sup>, P. Leblanc<sup>1</sup>, S. Holé<sup>2</sup>, T. Paillat<sup>1</sup>

<sup>1</sup>Institut Pprime, Université de Poitiers, France

<sup>2</sup>Laboratoire de Physique et d'Etude des Matériaux,  
Sorbonne Université, ESPCI Paris PSL Université, CNRS, France

**Abstract** — The presence of electric charges within liquid is relatively unexplored despite its role in electrochemical energy storage and industrial safety. Quantifying charge distribution in liquids and at solid/liquid interfaces is therefore crucial to the efficiency and longevity of devices. Over time, metrologies using stimulus to measure space charges in solids have been transposed to liquids. The stimulus disturbs electrostatic equilibrium to induces electrical response. This study builds upon measuring electric charges in the Electrical Double Layer (EDL) using the Pressure-Wave-Propagation (PWP) method. It presents how the pressure wave amplitude, the liquid conductivity and the liquid nature impact the electrical response.

**Keywords**— Space Charges, PWP method, Electrical Double Layer, Interface

## I. INTRODUCTION

When a solid and a liquid come into contact, poorly understood electrochemical phenomena electrically polarize the interface to form a charge distribution known as the electrical double layer (EDL). This distribution is generally divided into two layers of charge: a first layer located within the solid and a second layer of opposite polarity located inside the liquid, while maintaining electroneutrality. Several models have been developed to describe the EDL, including the Stern model [1], which remains one of the most commonly accepted. This model is based on a charge creation mechanism through an adsorption process related to the chemical nature of solid and liquid. Even a few parts per million of impurities in the liquid are sufficient to significantly alter the properties of the EDL.

In the field of electrical engineering, particularly for power components such as power transformers cooled by a flow of a dielectric liquid, the EDL is a major concern for industrial professionals as it can lead to electrostatic hazard. Indeed, when the liquid is set in motion, it carries one part of the electric charges present in the liquid and disrupts the electrical double layer balance. To restore its electrostatic equilibrium, new charges are generated at the interface, which can lead to localized increases in electrical potential, such as in the case of metallic conductors or dielectrics. In some cases, these local potential increases can reach the dielectric breakdown of the material which is at risk for the equipment.

Quantifying and determining the distribution of charges within liquids and at solid/liquid interfaces are therefore essential to prevent such risks.

In the field of energy, especially in energy storage, both supercapacitors and electrochemical batteries play a key role in facilitating the integration of intermittent renewable energy sources. These systems operate based on the transfer of electrical charges at solid-liquid interfaces and on the Electric Double Layer (EDL). The liquids employed are conductive fluids or electrolytes. A thorough comprehension of the organization of electric charge distribution within the liquid is equally crucial to optimize and ensure the reliability of these devices.

Various experimental techniques have been used to study the EDL, such as flow electrification [2-3] or using the Kerr effect [4]. However, these techniques indirectly provide information about the charge distribution of the EDL through modeling that relies on various unverified assumptions. Recently, methods used for measuring space charges in solids have been adapted for charge measurement in liquids, such as the thermal step method (TSM) [5], the pulsed electro-acoustic (PEA) method [6] and the pressure wave propagation (PWP) method [7].

This work builds upon previous research conducted on PWP method [7-8]. Its objective is to present the latest advancements in measurement techniques and the analysis of electrical measurement signals for interfaces between conductive solids and more and less conductive liquids.

---

Corresponding author: Valentin BERRY  
e-mail address: valentin.berry@univ-poitiers.fr

## II. THEORETICAL APPROACH

### A. Electrical double layer description

The electrical double layer can be likened to an electrical capacitor, with the solid acting as one electrode and the liquid as the other electrode. According to Stern (Fig. 1), the charges in the solid are uniformly distributed on the first atomic layers, while the charges in the liquid undergo the diffusion and are distributed deeper into the liquid. At equilibrium, the space charge density is highest at the interface ( $\rho_w$ ) and decreases exponentially towards the liquid bulk until it becomes zero. The thickness of this charge distribution is conventionally referred to as the Debye length  $\delta_0$  (1) [9], which is determined only by the electrical properties of the liquid including the permittivity  $\epsilon$ , the conductivity  $\sigma$  and the average diffusion coefficient of charged species in the liquid  $D_0$ . According to this model, 95% of the charges in the liquid are located near to the interface in a thickness of  $3\delta_0$ . For conductive liquids (aqueous solutions),  $\rho_w$  is approximately equal to  $10^4 \text{ C}\cdot\text{m}^{-3}$  with  $\delta_0$  of a few angstroms, while for dielectric liquids (mineral oils, heptane), its order of magnitude is around  $10^{-4} \text{ C}\cdot\text{m}^{-3}$  with  $\delta_0$  that can reach millimeters [3].

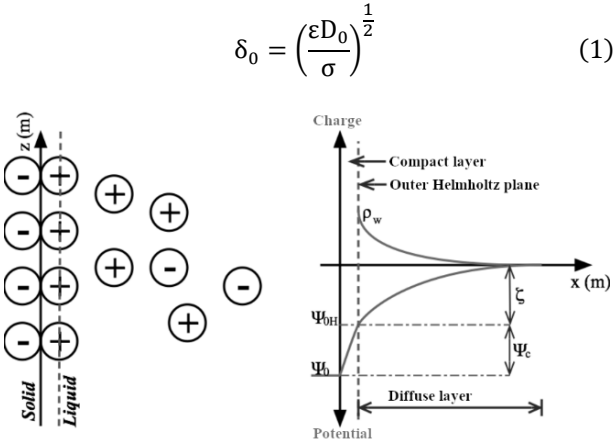


Fig. 1. Stern model description.

### B. PWP method

The Pressure Wave Propagation (PWP) method was developed by Laurenceau in 1976 for measuring space charges in solids [10]. It involves generating a planar pressure wave that propagates through the studied material, destabilizing the electrostatic equilibrium of charges and inducing a measurable electrical response (current or voltage) through a set of electrodes (Fig. 2) [11-12]. The pressure wave can be generated either by a laser pulse (Laser-Induced Pressure Pulse, LIPP) [13] or by a piezoelectric actuator (Piezoelectrically-Induced Pressure Pulse, PIPP) [14].

In planar geometry, the generated current response  $i_{\text{PWP}}(t)$  (2) [15] depends on the properties of the pressure stimulus  $P(x,t)$  through the strain wave  $S(x,t)$ , the

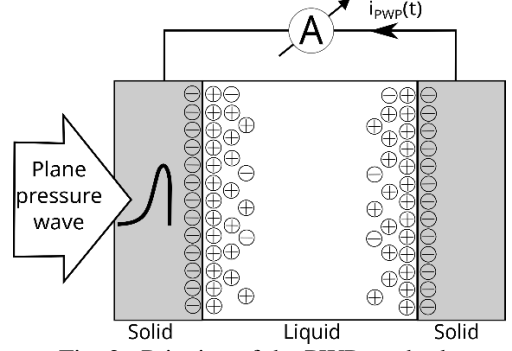


Fig. 2. Principle of the PWP method.

capacitance of the excited part of the sample  $C_0$ , the physical properties of the liquid such as permittivity  $\epsilon$ , electrostrictive coefficients  $a$ , and, the charge distribution  $\rho(x)$  in the medium through the distribution of the electric field  $E(x)$  via Maxwell-Gauss equation (3).

$$i_{\text{PWP}}(t) = -C_0 \int \left(1 - \frac{a}{\epsilon}\right) E(x) \frac{\partial S(x,t)}{\partial t} dx \quad (2)$$

$$\frac{d(\epsilon(x)E(x))}{dx} = \rho(x) \quad (3)$$

The strain  $S(x,t)$  is the derivative over space of the matter displacement of position  $x$  and time  $t$ . As the derivative over time of the displacement is the speed, it is interesting to replace  $\partial S(x,t)/\partial t$  in (2) by  $\partial V(x,t)/\partial x$  where  $V(x,t)$  is the speed of which the matter displaces in other words. Using the Maxwell-Gauss equation (3) and assuming a uniform material, the  $i_{\text{PWP}}(t)$  current is defined as a function of the charge distribution  $\rho(x)$  by (4).

$$i_{\text{PWP}}(t) = \frac{C_0}{\epsilon} \left(1 - \frac{a}{\epsilon}\right) \int \rho(x) V(x,t) dx \quad (4)$$

## III. PRINCIPLE OF PWP MEASUREMENT IN LIQUIDS

### A. Experimental setup

The measurement cell (Fig. 3) comprises an electrical control unit coupled with a high DC voltage power supply (Stanford PS35) that supplies the level of the excitation voltage  $V_{\text{ex}}$ . This configuration enables the generation of a rapid voltage drop (Fig. 4) across a piezoelectric actuator resulting in the induction of a planar pressure pulse. The electrical control unit consists of a gate driver ICs for high-voltage transistor GaN power switches (CoolGaN™) driven in a hard-switched mode. The GaN used enables ultra-fast switching for the excitation voltage  $V_{\text{ex}}$  up to 600 V. The print circuit board have been designed to ensure the good noise immunity and minimize the parasitic inductances at high frequency. The piezoelectric transducer is made of PZ24 ceramic [16], and has a circular shape with a diameter of 1.5 cm. With a thickness of 200  $\mu\text{m}$ , it is capable of generating short-duration

pressure pulses, leading to improved measurement resolution, while maintaining mechanical durability.

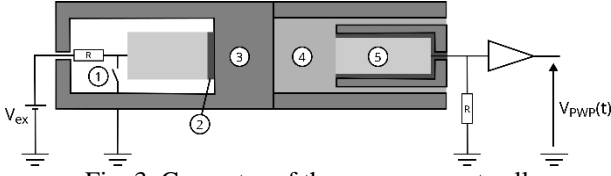


Fig. 3. Geometry of the measurement cell  
(1: Electrical control unit, 2: Piezoelectric actuator, 3: Waveguide electrode, 4: Liquid volume, 5: Measurement electrode).

Figures 4 and 5, which are the result of averaging over 1000 consecutive excitations at a frequency of 100 Hz, illustrate the electrical excitation  $V_{ex}$  generated by the electronic board for three different levels of excitation voltage, along with the corresponding induced pressure waves. The control voltage transitions from  $V_{ex}$  to 0 V in 30 ns, with a constant fall time  $t_{ex}$  independent of the amplitude (in the voltage range studied the variation of  $t_{ex}$  is smaller than 3 ns due to the variation of temperature of electronic components). Because the variation of the voltage applied on the piezoelectric actuator is decreasing, this actuator generates negative pressure wave. This pressure wave (Fig. 5) exhibits a relatively symmetrical shape during its decay and growth phases, with a slight rebound observed at the end. This bounce is probably attributed to oscillations around 0 V in the applied voltage to the piezoelectric actuator (Fig. 4). The amplitude of the wave increases proportionally with the excitation level, reaching 6 MPa, while its duration  $\tau$  remains completely independent of the excitation level as confirmed by dimensionless study (Fig. 6). Calculated at 50 % of the maximum pressure value, the duration of the pressure wave is 34.88 ns. S. Holé [17], who pioneered this principle of stimulus generation for measurement in solids, theoretically established the shape of the pressure wave based on the electrical excitation and verified its consistency with experimental measurements. It was also demonstrated that the measurement resolution is linked to the propagation velocity of the pressure wave  $v$  and its bandwidth ( $f_{max}$ ) according to Equation (5) [18].

$$R = \frac{v}{2f_{max}} \quad (5)$$

According to S. Holé [19], two types of resolutions should be considered. The positioning  $R_p$  and discerning  $R_D$  resolutions. The first emphasizes the positioning of the charge within the sample, while the second reflects the ability to discriminate between two separate charges. For an elastic pressure wave, they are given respectively by:

$$R_p = \frac{0.98v\tau}{SNR} \quad (6)$$

$$R_D = \frac{1.68v\tau}{\sqrt{SNR}} \quad (7)$$

where SNR is the signal-to-noise ratio. In this paper, the resolution calculated is  $R_D$  which is similar to  $R$  keeping SNR to the one of measurements.

The generated pressure wave propagates through the aluminum waveguide (3), which also serves as the excitation electrode, then into the liquid volume (4), and finally into the brass measurement electrode (5). The voltage signal  $V_{PWP}(t)$  obtained between the two electrodes is amplified by 60 dB (Analog Modules 322-12-50) and is digitized using a Tektronix® MSO64B oscilloscope. The voltage signal is directly related to the current  $i_{PWP}(t)$  through the 50  $\Omega$  input impedance of the amplifier. The electrical excitation  $V_{ex}$  can be adjusted in amplitude from 30 to 200 V and modulated in frequency up to 1 kHz. The interelectrode spacing ( $d$ ) can be adjusted from 0 to 3 mm and is controlled by a micrometer screw within a 1  $\mu$ m uncertainty.

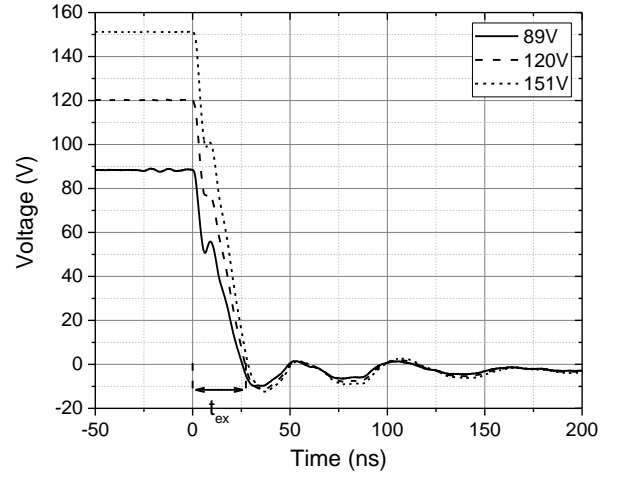


Fig. 4. Applied voltage on piezoelectric actuator for different excitation voltages  $V_{ex}$ .

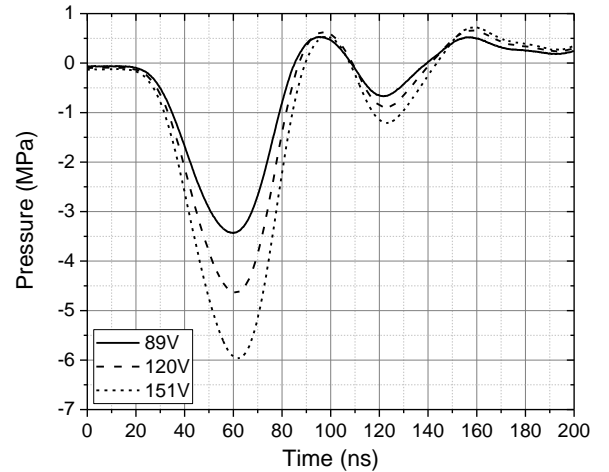


Fig. 5. Pressure wave profile generated for the three levels of excitation in Figure 4.

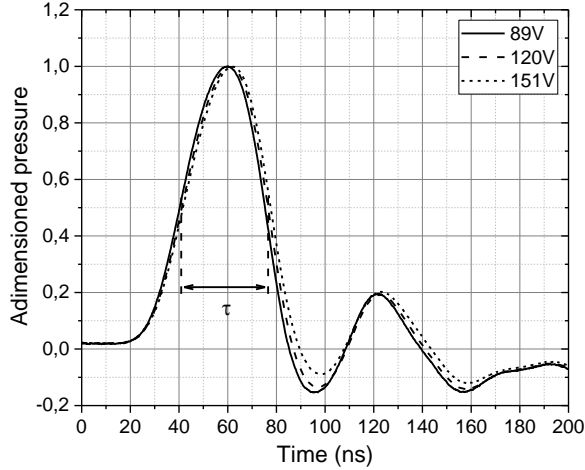


Fig. 6. Normalized pressure wave profile generated for the three levels of excitation in Figure 4 (normalization established with the maximum value of the pressure wave).

### B. Electric properties of the different liquids

Different liquids with varying levels of conductivity have been examined. They are either of different chemical nature in their pure state (water, glycerol and ethanol), or modified by the addition of additives. KOH 0.001M corresponds to a base of water with 0.001M of potassium hydroxide (KOH). In the case of pure glycerol, a saltwater solution with 32 ppm of NaCl is added at different concentrations to vary the conductivity of the mixture. The conductivity and permittivity properties of each solution were measured using impedance spectroscopy (AMETEK® Modulab XM CHAS 08) and summarized in Table I. To conduct the studies when the electrical double layer is at the equilibrium, fully developed [20], the relaxation time of electric charges in the liquid is determined based on the liquid properties:

$$\tau_r = \frac{\epsilon}{\sigma} \quad (8)$$

For the estimation of the Debye length (1), the diffusion coefficient  $D_0$  has also been measured for various liquids using impedance spectroscopy [21] and compared to bibliography data [22-24].

### C. Typical recording of the signal

Before conducting the measurements, empty tests (without liquid) were performed to qualify the cell. Regardless of the inter-electrode spacing and excitation voltage level, the measured signal present only a background noise below 0.1 mV.

The measured signals are the result of averaging over 1000 consecutive acquisitions at a frequency of 100 Hz. This frequency is sufficiently low to allow the EDL to re-equilibrate between two successive excitations, considering the relaxation time (Table I). Each

measurement is repeated 5 times for an estimated reproducibility error of less than 8 %. Figure 7 shows a typical recording of the electrical voltage signal  $V_{PWP}(t)$  obtained in the cell for ethanol when  $V_{ex} = 110V$ . It is characterized by two sets of transients.

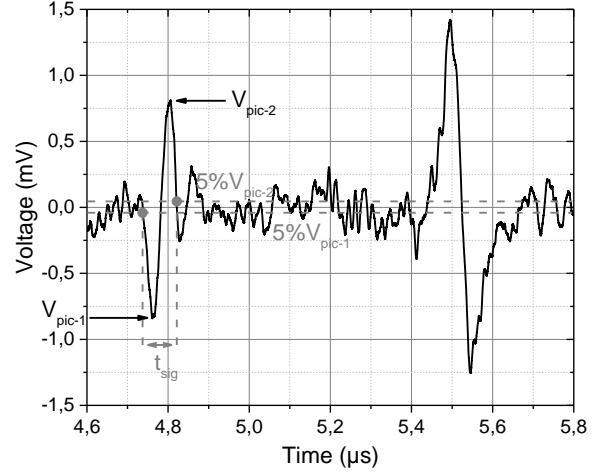


Fig. 7. Electrical response obtained at aluminum/Gly0 and at Gly0/brass interfaces for  $V_{ex} = 110V$ .

The first consists of a negative peak followed by a positive peak, appearing  $4.75 \mu s$  after the excitation of the piezoelectric element. This represents the electrical response induced by the first interface once the pressure pulse has traveled through the waveguide. The second part of the signal occurs 600 nanoseconds later and corresponds to the second interface, once the pressure has crossed the sample. This time, it consists of a positive peak followed by a negative peak. This sign inversion in the electrical responses is consistent. Indeed, the first interface is excited by the pressure wave from the solid (aluminum) to the liquid (glycerol), while the second interface is excited from the liquid to the solid (brass). The differences in amplitude between the two signatures are likely due to the differences in nature between the two interfaces as well as the pressure wave is partially reflected at the back electrode. The time interval between these two sets of signals precisely corresponds to the propagation velocity of the pressure wave in glycerol ( $v = 1998 m \cdot s^{-1}$ ) through the 1 mm inter-electrode spacing.

## IV. RESULTS AND DISCUSSIONS

In the following sections of this paper, the analysis of the electrical response is exclusively focused on the transient of the first interface (solid/liquid). At this interface, the electrical signal is probably not disturbed by any reflections of the pressure wave. The analysis concedes the amplitude of the first and second peaks ( $V_{peak-1}$  and  $V_{peak-2}$ ) as well as the duration of the signal signature  $t_{sig}$  obtained between 5 % of  $V_{peak-1}$  and 5 % of  $V_{peak-2}$  as shown on Fig. 7. The peaks following these two peaks are not considered since they are replicas.

Table I

Electrical properties of the different liquids.

The « Gly0 » solution corresponds to pure glycerol, while the others are glycerol-based additive solutions.

Sol.	$\epsilon_r$	$\sigma$ (S.m <sup>-1</sup> )	$\nu$ (ms <sup>-1</sup> )	$D_0$ (m <sup>2</sup> s <sup>-1</sup> )	$\delta_0$ ( $\mu$ m)	$\tau_r$ ( $\mu$ s)	$R_D$ ( $\mu$ m)
KOH 0.001M	75.09	$1.83 \cdot 10^{-2}$	$1.55 \cdot 10^3$	$1.64 \cdot 10^{-2}$	24.43	0.04	9.79
Water	102.07	$4.11 \cdot 10^{-4}$	$1.45 \cdot 10^3$	$1.70 \cdot 10^{-4}$	19.34	2.20	20.26
Ethanol	27.53	$7.81 \cdot 10^{-6}$	$1.54 \cdot 10^3$	$4.76 \cdot 10^{-7}$	14.86	31.19	19.89
Gly0	53,24	$6,54 \cdot 10^{-7}$	$1.99 \cdot 10^3$	$3.95 \cdot 10^{-6}$	53.25	721.02	31.91
Gly1	51,69	$7,54 \cdot 10^{-7}$	$1.97 \cdot 10^3$	$4.73 \cdot 10^{-6}$	53.52	606.56	30.69
Gly2	53,85	$9,74 \cdot 10^{-7}$	$1.94 \cdot 10^3$	$3.43 \cdot 10^{-6}$	40.92	489.33	27.19
Gly3	52,64	$9,93 \cdot 10^{-7}$	$1.95 \cdot 10^3$	$1.79 \cdot 10^{-5}$	91.71	469.32	25.24
Gly4	53,30	$1,71 \cdot 10^{-6}$	$1.96 \cdot 10^3$	$5.67 \cdot 10^{-6}$	39.57	276.27	25.42
Gly5	54.59	$2.52 \cdot 10^{-6}$	$1.96 \cdot 10^3$	$7.13 \cdot 10^{-6}$	36.95	191.36	23.75
Gly6	59.72	$1.55 \cdot 10^{-5}$	$1.98 \cdot 10^3$	$2.84 \cdot 10^{-4}$	98.48	34.15	20.39

### A. Variation of the pressure wave amplitude.

Figure 8 shows the variation of  $V_{PWP}(t)$  as a function of the potential  $V_{ex}$  for the Gly6 liquid at 20°C. Increasing the voltage amplitude results in an increase in the stimulus without altering its temporal behavior.

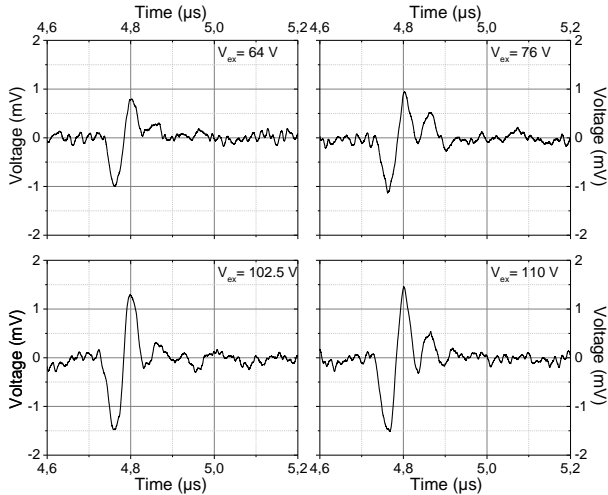


Fig. 8. Electrical signal at the first interface for different values of  $V_{ex}$  (64, 76, 102.5 and 110 V).

This observation is particularly evident when analyzing the amplitude of the peaks  $V_{peak-1}$  and  $V_{peak-2}$ , which appear to vary linearly and in the same proportions as  $V_{ex}$  (Fig. 9). This suggests that when  $V_{ex}$  increases linearly, both the pressure wave amplitude and the voltage  $V_{PWP}(t)$  increase in the same way.  $t_{sig}$  (Fig. 10) appears to be independent of the excitation voltage within the studied range, with a relatively significant measurement uncertainty (6 %) due to the noise in the signal. The behavior of the impact on the variation of pressure wave amplitude on the electrical response is confirmed by a numerical study [25].

Furthermore, considering the shape of the pressure wave induced by the piezoelectric and the results of the

numerical study [25], this signature of two peaks in the signal, negative for the first and for positive the second, can only be attributed to an electrical double layer composed of negative charges in the solid and positive charges in the liquid.

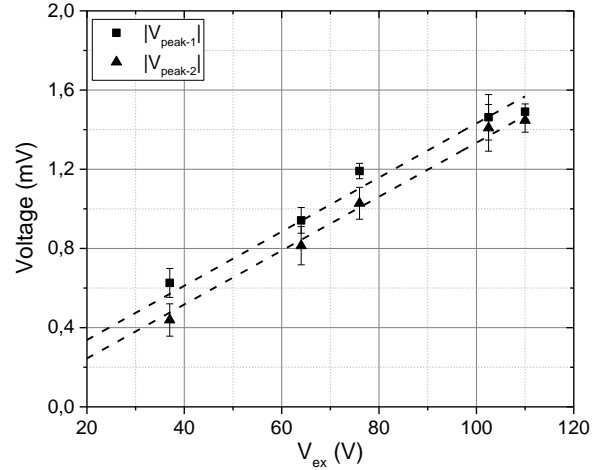


Fig. 9. Amplitude of the first voltage peaks as a function of  $V_{ex}$ .

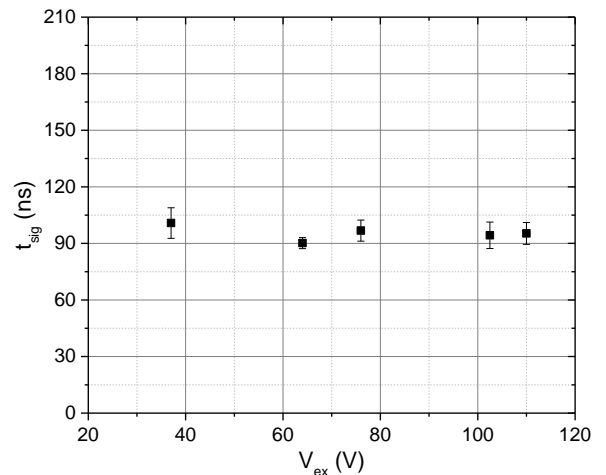


Fig. 10. Duration of the signal at the first interface as a function of  $V_{ex}$ .

### B. Impact of the liquid conductivity

Figure 11 shows the temporal evolution of  $V_{PWP}(t)$  for different conductivities at  $V_{ex} = 110V$ . An increase in conductivity  $\sigma$  leads to an increase of the voltage amplitude without affecting significantly its temporal behavior.

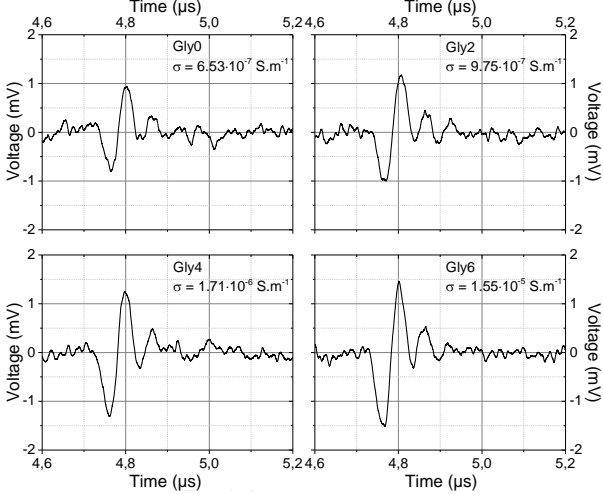


Fig. 11. Electrical response at solid/liquid interface for « Gly0 », « Gly2 », « Gly4 » and « Gly6 » solutions for  $V_{ex} = 110V$ .

The amplitudes of the peaks  $V_{peak-1}$  and  $V_{peak-2}$  exhibit an increasing exponential progression and are influenced in the same proportions (Fig. 12). The increase in conductivity results in a significant increase in the amplitudes of the different peaks, on the order of 175% between  $10^{-7}$  and  $5 \cdot 10^{-6} S.m^{-1}$ . Above this range, the amplitudes of the peaks tend to approach a constant value. This overall behavior is likely due to the antagonistic effects of increasing conductivity [25]. On one hand, increasing the liquid conductivity, increases the space charge density of the EDL [5] and promotes  $V_{PWP}$ , while on the other hand, it reduces the thickness of the diffuse layer and tends to decrease  $V_{PWP}$  [25]. In the studied conductivity range, especially at low values, the increase in space charge density appears to dominate.

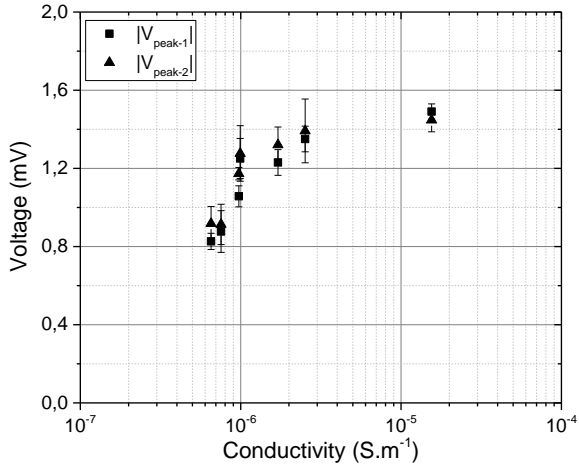


Fig. 12. Amplitude of the first voltage peaks as a function of solution conductivity.

Furthermore, as long as the thickness of the diffuse layer is higher than the spatial resolution  $R_D$  (Table I),  $t_{sig}$  evolves according to  $\delta_0$  as predictable by numerical study [25]. This behavior is visible on the first points in Fig. 13. On the last points, when the value of  $\delta_0$  is similar or smaller than the spatial resolution,  $t_{sig}$  seems to be constant. Then, when the spatial resolution is similar or higher than  $\delta_0$  some loss of information distorts the measurement.

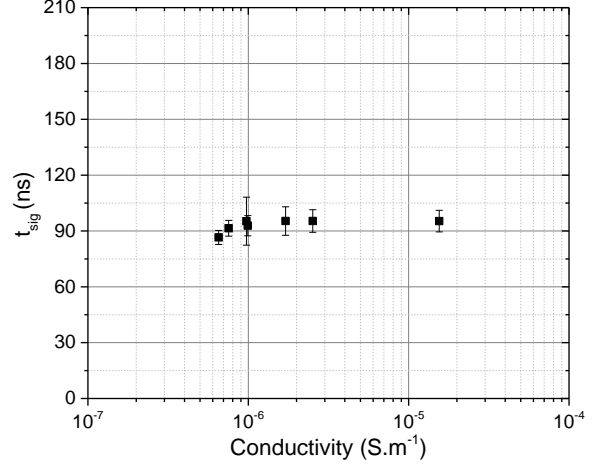


Fig. 13. Duration of the signal at the first interface as a function of solution conductivity.

### C. Impact of the liquid nature.

Figure 14 illustrates the temporal evolution of  $V_{PWP}(t)$  for four different liquids excited by a pressure wave generated for  $V_{ex} = 75V$  with an inter-electrode spacing fixed at 1 mm. Regardless of the studied liquid,  $V_{PWP}$  presents a specific temporal shape, with amplitude and signal duration unique to each liquid. Depending on the nature of the liquid, the signature of  $V_{PWP}$  evolves. The first peak is positive, and the second peak is negative for KOH 0.001M and water, while it is the opposite for ethanol and glycerol.

This behavior can mainly be attributed to a polarization inversion at the solid/liquid interface and the electrochemical reactions which occur at the interface. According to (4) and because the pressure wave is negative the electric charge distribution would be negative in the solid and positive in the liquid for the aluminum/KOH and aluminum/water couples, and vice versa for the other couples.

In line with the previous findings, the signal amplitude is significantly influenced by the liquid's conductivity, increasing with it (Fig. 15). However, the signal duration is less sensitive to these variations (Fig. 16, 17) as the ratio between the extent of the pressure wave and  $\delta_0$  is similar for the different liquids. Regardless of the liquids studied, the thickness of the diffuse layer ( $3\delta_0$ ) remains well higher than the measurement resolution (Table 1).

Finally, the signal-to-noise ratio appears to be quite dependent on the liquid. However, given the current

understanding of the measurement, no interpretation can be proposed at this stage.

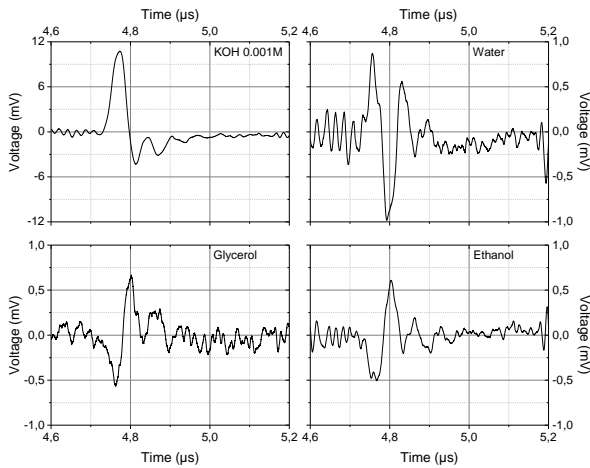


Fig. 14. Electrical response at aluminum and different liquid interfaces (KOH solution, Water, Glycerol, Ethanol) at  $V_{ex} = 75V$ .

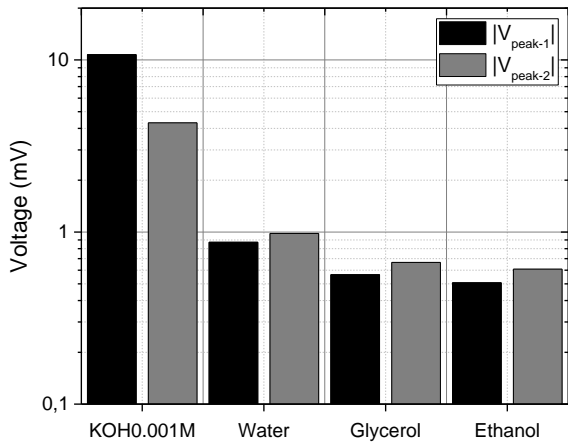


Fig. 15. Absolute value of the two first peaks of the electrical response at the aluminum/liquid interface for the different solutions studied at  $V_{ex} = 75V$ .

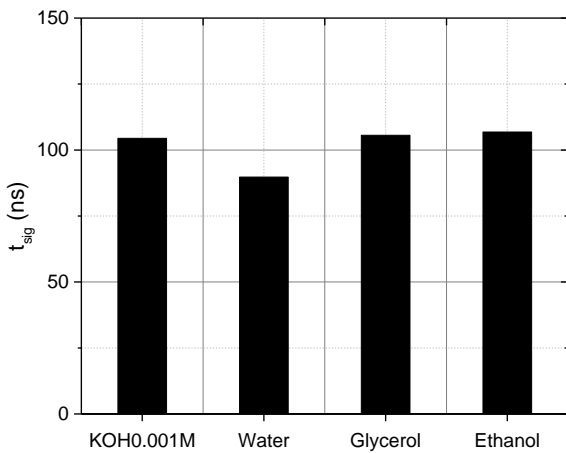


Fig. 16. Duration  $t_{sig}$  of the signal at the first interface as a function of the different liquids studied.

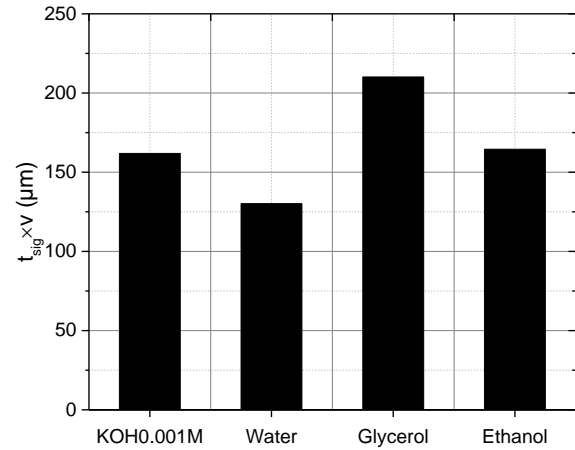


Fig. 17. Spatial extent of the signal at the first interface as a function of the different liquids studied.

## V. CONCLUSION

This adaptation of space charge measurement using PWP method to solid/liquid interfaces appear particularly promising. For the range of conductive liquids used, a consistent signal has always been measured. It is specific to the interface properties, exhibiting different amplitudes and dynamics. All these measurements are limited by the sensitivity and resolution of the measurement. Sensitivity can be improved by increasing the excitation voltage. As for resolution, it is more delicate to enhance as it depends on the choice of the piezoelectric material and thickness, as well as the speed of voltage drop.

## ACKNOWLEDGEMENTS

This work is supported by the "Investissement d'Avenir" program (LABEX INTERACTIF, reference ANR-11 LABX-0017-01), "Region Nouvelle-Aquitaine" and the PLATABAT project (2022-23222510).

## REFERENCES

- [1] Stern, O., 1924. Zur Theorie Der Elektrolytischen Doppelschicht. Zeitschrift für Elektrochemie und angewandte physikalische Chemie 30, 508–516. <https://doi.org/10.1002/bbpc.192400182>
- [2] Moreau, E., Paillat, T., Touchard, G., 2001. Space charge density in dielectric and conductive liquids flowing through a glass pipe. Journal of Electrostatics 51–52, 448–454. [https://doi.org/10.1016/S0304-3886\(01\)00082-1](https://doi.org/10.1016/S0304-3886(01)00082-1)
- [3] Paillat, T., Moreau, E., Touchard, G., 2001. Space charge density at the wall in the case of heptane flowing through an insulating pipe. Journal of Electrostatics 53, 171–182. [https://doi.org/10.1016/S0304-3886\(01\)00139-5](https://doi.org/10.1016/S0304-3886(01)00139-5)
- [4] Jian Shi, Qing Yang, Wenxia Sima, Lei Liao, Sisi Huang, Zahn, M., 2013. Space charge dynamics investigation based on Kerr electro-optic measurements and processing of CCD images. IEEE Trans. Dielect. Electr. Insul. 20, 601–611. <https://doi.org/10.1109/TDEI.2013.6508764>
- [5] Sidambarompou, X., Laurentie, J.-C., Notinger, P., Paillat, T., Leblanc, P., Touchard, G., Tourelle, A., Guille, O., 2019. A Non-destructive Thermal Stimulus Method as

- a Tool for studying the Electrical Double Layer, in: 2019 IEEE 20th International Conference on Dielectric Liquids (ICDL), IEEE, Roma, Italy, pp. 1–4. <https://doi.org/10.1109/ICDL.2019.8796837>
- [6] Wu, K., Zhu, Q., Wang, H., Wang, X., Li, S., 2014. Space charge behavior in the sample with two layers of oil-immersed-paper and oil. *IEEE Trans. Dielect. Electr. Insul.* 21, 1857–1865. <https://doi.org/10.1109/TDEI.2014.004241>
- [7] Ndour, A., Holé, S., Leblanc, P., Paillat, T., 2021. Direct observation of electric charges at solid/liquid interfaces with the pressure-wave-propagation method. *Journal of Electrostatics* 109, 103527. <https://doi.org/10.1016/j.elstat.2020.103527>
- [8] Lewiner, J., Hole, S., Ditchi, T., 2005. Pressure wave propagation methods: a rich history and a bright future. *IEEE Trans. Dielect. Electr. Insul.* 12, 114–126. <https://doi.org/10.1109/TDEI.2005.1394022>
- [9] Touchard, G., 2001. Flow electrification of liquids. *Journal of Electrostatics* 51–52, 440–447. [https://doi.org/10.1016/S0304-3886\(01\)00081-X](https://doi.org/10.1016/S0304-3886(01)00081-X)
- [10] Laurenceau, P., Dreyfus, G., Lewiner, J., 1977. New Principle for the Determination of Potential Distributions in Dielectrics. *Phys. Rev. Lett.* 38, 46–49. <https://doi.org/10.1103/PhysRevLett.38.46>
- [11] Cheng, L., Zhong, L., Zhang, Y., Tan, S., Chen, J., 2009. A Piezo-PWP method for charge measurement of the cell suspension, in: 2009 IEEE 9th International Conference on the Properties and Applications of Dielectric Materials (ICPADM), IEEE, Harbin, China, pp. 907–910. <https://doi.org/10.1109/ICPADM.2009.5252243>
- [12] Takada, T., 1999. Acoustic and optical methods for measuring electric charge distributions in dielectrics. *IEEE Trans. Dielect. Electr. Insul.* 6, 519–547. <https://doi.org/10.1109/TDEI.1999.9286758>
- [13] Alquie, C., Dreyfus, G., Lewiner, J., 1981. Stress-Wave Probing of Electric Field Distributions in Dielectrics. *Phys. Rev. Lett.* 47, 1483–1487. <https://doi.org/10.1103/PhysRevLett.47.1483>
- [14] Eisenmenger, W., Haardt, M., 1982. Observation of charge compensated polarization zones in polyvinylidenefluoride (PVDF) films by piezoelectric acoustic step-wave response. *Solid State Communications* 41, 917–920. [https://doi.org/10.1016/0038-1098\(82\)91235-2](https://doi.org/10.1016/0038-1098(82)91235-2)
- [15] Holé, S., Ditchi, T., Lewiner, J., 2000. Influence of divergent electric fields on space-charge distribution measurements by elastic methods. *Phys. Rev. B* 61, 13528–13539. <https://doi.org/10.1103/PhysRevB.61.13528>
- [16] Piezoelectric ceramic Pz 24 from Ferroperm A/S.
- [17] Holé, S., Lewiner, J., 1996. Single transducer generation of unipolar pressure waves. *Appl. Phys. Lett.* 69, 3167–3169. <https://doi.org/10.1063/1.116817>
- [18] Dagher, Hole, Lewiner, 2006. A preliminary study of space charge distribution measurements at nanometer spatial resolution. *IEEE Trans. Dielect. Electr. Insul.* 13, 1036–1041. <https://doi.org/10.1109/TDEI.2006.247829>
- [19] Hole, S., 2008. Resolution of direct space charge distribution measurement methods. *IEEE Trans. Dielect. Electr. Insul.* 15, 861–871. <https://doi.org/10.1109/TDEI.2008.4543124>
- [20] Maatschappij, K.N.P., Klinkenberg, A., van der Minne, J.L., 1957. *Electrostatics in the Petroleum Industry: The Prevention of Explosion Hazards*. A Royal Dutch-Shell Research and Development Report. Elsevier Publishing Company.
- [21] Sidambarompoulé, X., Notinger, P., Paillat, T., Laurentie, J.-C., Leblanc, P., 2020. Study of electrical properties and estimation of average mobility and diffusion coefficients in several insulating liquids by dielectric spectroscopy.
- [22] Hills, E.E., Abraham, M.H., Hersey, A., Bevan, C.D., 2011. Diffusion coefficients in ethanol and in water at 298K: Linear free energy relationships. *Fluid Phase Equilibria* 303, 45–55. <https://doi.org/10.1016/j.fluid.2011.01.002>
- [23] Agmon, N., 1995. The Grotthuss mechanism. *Chemical Physics Letters* 244, 456–462. [https://doi.org/10.1016/0009-2614\(95\)00905-J](https://doi.org/10.1016/0009-2614(95)00905-J)
- [24] Ternström, G., Sjöstrand, A., Aly, G., Jernqvist, Å., 1996. Mutual Diffusion Coefficients of Water + Ethylene Glycol and Water + Glycerol Mixtures. *J. Chem. Eng. Data* 41, 876–879. <https://doi.org/10.1021/je9501705>
- [25] Berry, V., Zheng, L., Leblanc, P., Hole, S., Paillat, T., 2023. Numerical study of the electric charge measurement by the Pulse Wave Propagation method: Application to the Electrical Double Layer, in: 2023 IEEE 22th International Conference on Dielectric Liquids (ICDL), IEEE, Worcester, USA, pp. 1–4. <https://doi.org/10.1109/ICDL59152.2023.10209316>